

This article was downloaded by: [Andriy Gusak]

On: 16 March 2015, At: 16:17

Publisher: Taylor & Francis

Informa Ltd Registered in England and Wales Registered Number: 1072954 Registered office: Mortimer House, 37-41 Mortimer Street, London W1T 3JH, UK



Philosophical Magazine

Publication details, including instructions for authors and subscription information:

<http://www.tandfonline.com/loi/tphm20>

Electromigration revisited: competition between Kirkendall shift and backstress in pure metals and two-phase alloys

A. Gusak^a, B. Wierzba^b & M. Danielewski^c

^a Department of Theoretical Physics, Cherkasy National University, Shevchenko Street 81, 18000 Cherkasy, Ukraine

^b Faculty of Mechanical Engineering and Aeronautics, Research and Development Laboratory for Aerospace Materials, Rzeszow University of Technology, al. Powstańców Warszawy 12, 35-959 Rzeszów, Poland

^c Physical Chemistry of Solids, AGH University of Science and Technology, Krakow, Poland

Published online: 13 Mar 2015.



CrossMark

[Click for updates](#)

To cite this article: A. Gusak, B. Wierzba & M. Danielewski (2015): Electromigration revisited: competition between Kirkendall shift and backstress in pure metals and two-phase alloys, *Philosophical Magazine*, DOI: [10.1080/14786435.2015.1020352](https://doi.org/10.1080/14786435.2015.1020352)

To link to this article: <http://dx.doi.org/10.1080/14786435.2015.1020352>

PLEASE SCROLL DOWN FOR ARTICLE

Taylor & Francis makes every effort to ensure the accuracy of all the information (the "Content") contained in the publications on our platform. However, Taylor & Francis, our agents, and our licensors make no representations or warranties whatsoever as to the accuracy, completeness, or suitability for any purpose of the Content. Any opinions and views expressed in this publication are the opinions and views of the authors, and are not the views of or endorsed by Taylor & Francis. The accuracy of the Content should not be relied upon and should be independently verified with primary sources of information. Taylor and Francis shall not be liable for any losses, actions, claims, proceedings, demands, costs, expenses, damages, and other liabilities whatsoever or howsoever caused arising directly or indirectly in connection with, in relation to or arising out of the use of the Content.

This article may be used for research, teaching, and private study purposes. Any substantial or systematic reproduction, redistribution, reselling, loan, sub-licensing, systematic supply, or distribution in any form to anyone is expressly forbidden. Terms &

Conditions of access and use can be found at <http://www.tandfonline.com/page/terms-and-conditions>

Electromigration revisited: competition between Kirkendall shift and backstress in pure metals and two-phase alloys

A. Gusak^a, B. Wierzbab* and M. Danielewski^c

^aDepartment of Theoretical Physics, Cherkasy National University, Shevchenko Street 81, 18000 Cherkasy, Ukraine; ^bFaculty of Mechanical Engineering and Aeronautics, Research and Development Laboratory for Aerospace Materials, Rzeszow University of Technology, al. Powstańców Warszawy 12, 35-959 Rzeszów, Poland; ^cPhysical Chemistry of Solids, AGH University of Science and Technology, Krakow, Poland

(Received 30 October 2014; accepted 6 February 2015)

The simple phenomenological model and analytical approach of electromigration in the two-phase alloy (solder) under combined influence of the Kirkendall effect, backstress and sedimentation is presented. It is compared with electromigration in pure metal under condition of quasi-equilibrium vacancies (unlimited power of vacancy sinks-sources) and electromigration in pure metal with account of nonequilibrium vacancies.

Keywords: electromigration; phase separation; ultra-high gravity; backstress; Kirkendall effect

1. Introduction

Already in 1948, Darken [1] referred to observation made by Schwarz [2], who had noticed that tungsten lamp filaments heated by direct current commonly fail by necking down near the positive end, with a simultaneous swelling at the position near the negative filament end. Schwarz explained this phenomenon by the motion of tungsten cations, which migrate in the high-temperature region from the positive end towards the negative end. Darken concluded that alloying elements in the tungsten may migrate. Nowadays, this phenomenon is known as electromigration, and produces failures of Al, Cu interconnects as well as solder joints and are the reason for constant attention to the details in this process.

The failure is a consequence of the existence of divergences in the transport of matter. It is caused by very high local current densities due to the small dimensions of the conducting lines in the integrated circuits, which can lead to significant values of atom transport. Improvements in the electromigration time to failure have been achieved empirically. With the continued drive for miniaturization, the electromigration failure remains a concern for integrated circuit manufacturers.

After the famous Blech experiment [3] and its elegant explanation by Nabarro [4], the ‘backstress’ became one of the most frequently used words in papers on electromigration. The force of electromigration, F_{em} , is based on the effective charge number concept:

*Corresponding author. Email: bwierzba@prz.edu.pl

$$\mathbf{F}_{em} = (z_{el}^* + z_{wd}^*)e\mathbf{E}, \quad (1)$$

where \mathbf{E} is a vector of electric field, e effective ionic charges and z_{el}^* and z_{wd}^* are regarded as nominal valence of the diffusing metal, when the dynamic screening effect is ignored and valence (charge number) represents the momentum exchange effect due to the *electron wind force*, respectively [5,6]. One can express electric field by local current, $\mathbf{j}(t, x)$, and resistivity, $\rho(x)$,

$$\mathbf{E} = \rho\mathbf{j} \quad (2)$$

and obtain the alternative form of the Equation (1):

$$\mathbf{F}_{em} = (z_{el}^* + z_{wd}^*)e\rho\mathbf{j} \quad (3)$$

or simply:

$$\mathbf{F}_{em} = z^*e\rho\mathbf{j}. \quad (4)$$

Below, we will use projections of all vectors on x -axis instead of vectors.

Very good review of electromigration and thermomigration can be found in Basaran's work. He showed that the thermomigration driving force when present is much larger than electromigration [7,8]. His group developed a new displacement–diffusion-coupled model using finite-element method. Their model takes into account the viscoplastic behaviour of solder alloys, vacancy concentration evolution and the electromigration process. The driving forces for diffusion consists of (1) vacancy concentration gradient, (2) electrical field forces, (3) stress gradient and (4) thermal gradient [9–12].

In the next sections, the simple electromigration model with analytical approach will be formulated based on the diffusion equation only. We have introduced the (i) vacancy concentration gradient, (ii) electrical field forces, (iii) stress gradient and (iv) lattice drift (Kirkendall movement).

2. Electromigration in pure metal under condition of quasi-equilibrium vacancies

The postulate of the quasi-equilibrium vacancies indicates that the high current densities, stresses, etc. do not affect vacancies concentration, which depends on the temperature only due to the unlimited power of vacancy sinks-sources. The established models of electromigration assume that it is a consequence of the steady-state condition providing volume conservation under current stressing. Namely, mechanical force of stress gradient acting on migrating i -atom (*backstress*, $F^\sigma = \Omega\partial\sigma/\partial x$ (Ω – molar volume; $\sigma = -p = 1/3Sp\sigma_{ik}$ – hydrostatic part of the stress tensor)). In a planar diffusion couple with concentration gradient along x -axis, one has:

$$\sigma_{xx} = \sigma_{xy} = \sigma_{xz} = 0, \quad \sigma_{yy} = \sigma_{zz} = \frac{1}{2}Sp\sigma_{ik} = \frac{3}{2}\sigma. \quad (5)$$

The stress fully compensates the electron wind and electric field forces and hence, makes the total atomic flux ($J = cB \sum_k F_k$, ($B = D^*/kT$ – mobility, c – concentration)) equal to zero:

$$\sum_k F_k = z^*e\rho j_x + \Omega\partial\sigma/\partial x = 0 \Rightarrow J_x = cB(z^*e\rho j_x + \Omega\partial\sigma/\partial x) = 0. \quad (6)$$

On the other hand, diffusion community has an alternative way of providing volume conservation: namely, it is a lattice drift (Kirkendall effect) caused by the vacancy flux divergence leading to dislocation climb and subsequently to the construction of extra-planes in the accumulation region and dismantling of atomic planes in the depleting region [1,13,14]. The atomic flux due to electron wind is directed from cathode to anode and generates the vacancy flux in the opposite direction. As a result, extraplanes should be ‘inserted’ within the anode region and dismantled within the cathode region. Thus, the whole lattice should move from anode to cathode, counteracting and offsetting the drift generated by electron wind [2]. Drift velocity, v , then is determined from the condition of zero flux at interfaces:

$$J_x = cBz^*e\rho j_x + cv = 0 \Rightarrow v = -Bz^*e\rho j_x. \quad (7)$$

Together with lattice, the inert markers should move from anode to cathode with the same velocity, Equation (7). And markers movement is observed in solder joints¹ [5,15–25]. It is evident that Equations (6) and (7) cannot be valid simultaneously.² Of course, it seems evident that one should take into account both effects of the electron wind counteraction. In this case, one should write (instead of Equations (5) and (6)):

$$J_x = cB(z^*e\rho j_x + \Omega\partial\sigma/\partial x) + cv. \quad (8)$$

In the closed system, Equation (8) becomes:

$$J_x = cB(z^*e\rho j_x + \Omega\partial\sigma/\partial x) + cv = 0. \quad (9)$$

Naturally, it is impossible now to determine both Kirkendall velocity and backstress from the single conservation constraint. Physically, one must distinguish the drift related to lattice shift (when all atoms move simultaneously with lattice) and the drift related to migration of individual atoms. Recently, in a very interesting paper [26], the authors investigated the competition of electromigration and creep (but not explicitly, considering the lattice shift as one more natural way of equalizing the total atomic flux to zero). They considered nonlinear creep, which is characteristic for low temperatures and relatively high deformation rates.

Here, we will consider conditions, typical for solder joints experiments – low creep rates and high temperatures (not far from melting), so that main mechanism of creep should be Nabarro–Herring bulk diffusive creep that is taken into account as a second term in parenthesis of Equation (8). Unfortunately, it is impossible to find two unknowns (stress gradient and lattice velocity) from one constraint of zero flux. An attempt of simultaneous analysis was recently presented by Turlo et al. [27], but the authors used the arbitrary fitting parameter. We extend their model and use the relation between divergence of drift velocity and the time derivative of hydrostatic stress as a missing link [28]. Namely, divergence of drift velocity is determined by the vacancy generation/annihilation rate $\left(\frac{N_V - N_V^{eq}}{\tau_V}\right)$, which means generation or annihilation of lattice sites. This means dilatation of alloy leading to stress:

$$\frac{\partial v}{\partial x} = -\frac{N_V - N_V^{eq}}{\tau_V} = -\frac{1}{K} \frac{\partial S p \sigma_{ik}}{\partial t}, \quad (10)$$

where K is a bulk modulus; N_V and N_V^{eq} are the vacancy molar ration and equilibrium vacancy molar ratio; τ_V denotes the relaxation time for vacancies. Similar relation for

grain boundary migration was suggested by Kirchheim [29]. Using hydrostatic tension as one-third of the spur of stress tensor, one obtains:

$$\frac{\partial \sigma}{\partial t} = \frac{1}{3} \frac{\partial S p \sigma_{ik}}{\partial t} = -\frac{K}{3} \frac{\partial v}{\partial x}. \quad (11)$$

Taking the spatial derivative of Equation (9), using Equation (11) and neglecting the very small variation of overall concentration, c , and of diffusivity, one gets:

$$B \left(0 + \Omega \frac{\partial^2 \sigma}{\partial x^2} \right) - \frac{3}{K} \frac{\partial \sigma}{\partial t} = 0 \quad \Rightarrow \quad \frac{\partial \sigma}{\partial t} = \frac{1}{3} K \Omega B \frac{\partial^2 \sigma}{\partial x^2} = D_{\sigma}^{\text{eff}} \frac{\partial^2 \sigma}{\partial x^2}, \quad (12)$$

where $D^{\text{eff}} = \frac{1}{3} K \Omega B = D^* \frac{K \Omega}{3 k T}$ is an effective diffusivity of the deformation field in the metal.

After solving diffusion equation for stress, Equation (12), under given boundary conditions, drift velocity is then found from Equation (9):

$$v(x) = -\frac{D^*}{k T} (\Omega \partial \sigma / \partial x + z^* e \rho j_x). \quad (13)$$

The solution obtained clearly depends on boundary conditions.

2.1. Analytical solution

To solve above equations, the non-dimensional variables are introduced, $\xi = x/l$, where l denotes the conductor length (distance between cathode and anode), thus:

$$\varphi \equiv l \frac{\partial}{\partial x} \left(\frac{\Omega \sigma}{k_B T} \right) = \frac{\partial}{\partial \xi} \left(\frac{\Omega \sigma}{k_B T} \right) \quad (14)$$

Thus, the following equations are solved:

$$\frac{\partial \varphi}{\partial t} = \left(\frac{D^*}{l^2} \frac{K \Omega}{3 k_B T} \right) \frac{\partial^2 \varphi}{\partial \xi^2}, \quad 0 < \xi < 1, \quad (15)$$

or with non-dimensional time $\tau \equiv \frac{D^*}{l^2} \frac{K \Omega}{3 k_B T} t$

$$\frac{\partial \varphi}{\partial \tau} = \frac{\partial^2 \varphi}{\partial \xi^2} \quad (14')$$

$$v(x) = -\frac{D^*}{l} \left(\varphi + l \frac{z^* e \rho j_x}{k T} \right), \quad (16)$$

with initial conditions: $\varphi(t = 0, \xi) = 0$, $\forall 0 < \xi < 1$, and with boundary conditions, which depend on whether the cathode or/and anode end are free or fixed.

If the end Σ is free, then the backstress there is absent, so that $\varphi(\Sigma) = 0$.

If, instead, the end Σ is fixed, then the Kirkendall shift at this end is zero: $v(\Sigma) = 0$, so that (according to Equation (15)), $\varphi(\Sigma) = -l \frac{z^* e \rho j_x}{k T}$.

The following data are used in computations: $a \equiv \frac{K \Omega}{3 k_B T} = 100$ and $b \equiv -l \frac{z^* e \rho j_x}{k_B T} = 10$. Since, the effective charge is typically negative (due to electron

wind effect), it means that technical current in our example is directed from left to right: anode end (plus) is left and cathode end is right (minus), electron wind directed to the left, compression is left, tension is right, Kirkendall shift (if any) is directed to the right (to the cathode).

Non-dimensional velocity

$$\tilde{v}(\xi) = \frac{l}{D^*} \frac{3k_B T}{K\Omega} v(x) = \frac{1}{a} \cdot (b - \varphi) \tag{15'}$$

is plotted in Figures 1–3.

We shall consider three main cases:

- (1) Both ends fixed: $v(t, 0) = v(t, L) = 0 \Leftrightarrow \varphi(t, \xi = 0) = \varphi(t, \xi = 1) = -l \frac{z^* e \rho j_x}{kT} = b$;

During the time interval of getting to asymptotic regime, markers have option to move, so that initial markers array will redistribute. Maximum Kirkendall shift occurs at the centre of the line. Of course, magnitude of redistribution depends on current density. During the asymptotic regime, all markers are immovable (Figure 1). It means that the initially uniform markers distribution will shift to the cathode end and stop.

- (2) One end fixed, another – free:
 - (a) Left (anode) end fixed, right (cathode) end free: $v(t, \xi = 0) = 0 \Rightarrow \varphi(t, \xi = 0) = -l \frac{z^* e \rho j_x}{kT}$; $\varphi(t, \xi = 1) = 0$.

During the nonstationary period (transition period to steady state), the markers move so that initial markers array will continue redistributing, gathering near the cathode end (Figure 2).

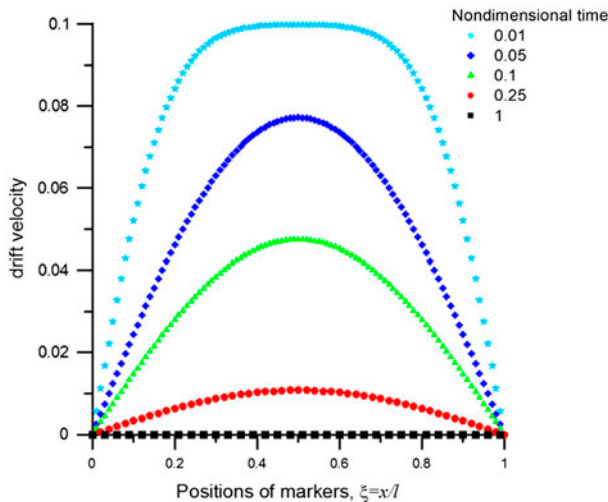


Figure 1. (colour online) The nondimensional velocity of markers drifts as a function of nondimensional coordinate, when both ends are fixed. Nondimensional time is introduced as $\tau \equiv \frac{D^*}{l^2} \frac{K\Omega}{3k_B T} t = \frac{D^*}{l^2} at$.

Markers will move to the right (cathode) end, the closer to the end, the faster the movement of the markers. At the end of the day, all markers should gather near the cathode end.

- (b) Left end free, right end fixed, Figure 3: $\varphi(t, \xi = 0) = 0; v(t, \xi = 1) = 0 \Rightarrow \varphi(t, \xi = 1) = -l \frac{z^* e \rho j_x}{kT}$

Markers will move from the left (anode) end to the right (cathode) end, the closer the markers are to the cathode end, the slower is the movement.

- (3) Both ends ‘almost’ free: $\varphi(t, \xi = 0) = 0; \varphi(t, \xi = 1) = 0, \frac{\partial \sigma}{\partial x}(t, 0) = \frac{\partial \sigma}{\partial x}(t, L) = 0$. The relative shift does not depend on position as can be seen from Equation (16):

$$v(x) = -\frac{D^*}{kT} z^* e \rho j_x, \quad \frac{\partial \sigma}{\partial x} = 0. \quad (17)$$

The last (exotic) case is the simplest one (although difficult for experimental realization): there is no backstress at all, only lattice drift according to Equation (7).

In [6,27], one can find the experimental results with the change of markers velocity sign near the anode end. Most probably, it is related to the fact of hillocks formation near the anode end and of current crowding – these factors were not included in our present analysis.

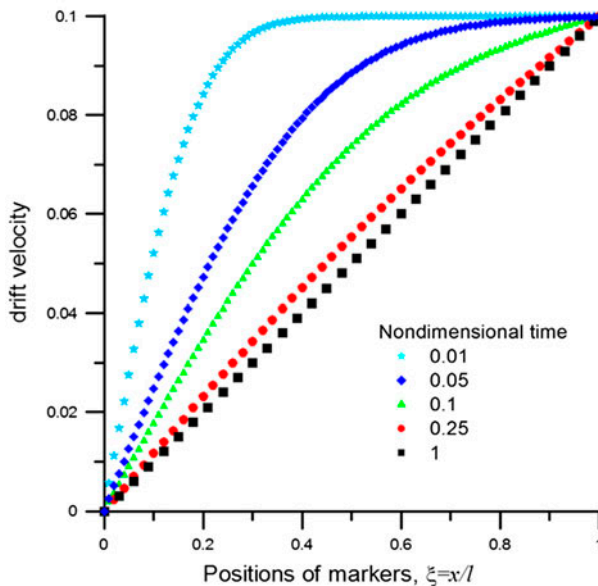


Figure 2. (colour online) The nondimensional drift velocity at various time moments in the case of left (anode) fixed end and right (cathode) free end.

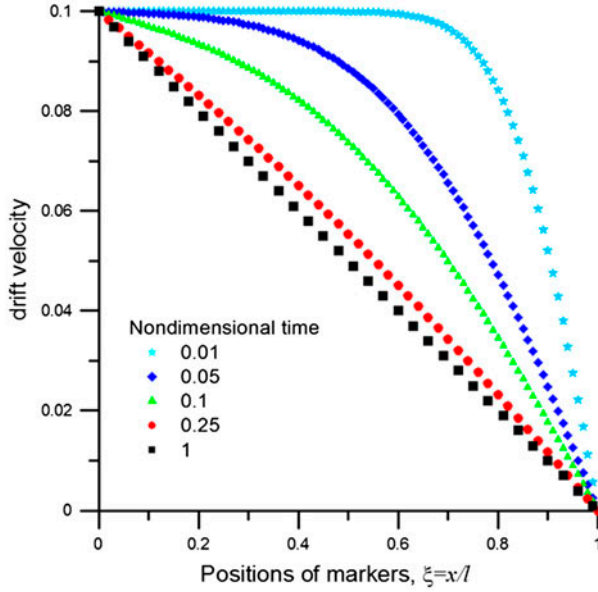


Figure 3. (colour online) The nondimensional drift velocity at various time moments in the case of left (anode) free end and right (cathode) fixed end.

3. Electromigration in pure metal with account of nonequilibrium vacancies

So far, we considered the case of powerful vacancy sinks-sources providing equilibrium vacancy concentration anywhere anytime. In reality, the power of vacancy sinks-sources can be taken into account by introducing the mean vacancy migration path L_V and corresponding vacancy relaxation time, $\tau_V = L_V^2/D_V$. If one neglects correlation factor, then $N_V D_V \cong D^*$.

Basic equations:

$$\begin{aligned} \Omega J_B &= \Omega j_B + (1 - N_V)v \\ &= \frac{(1 - N_V)D^*}{kT} \left(-Ze\rho j_x + \Omega \frac{\partial \sigma}{\partial x} \right) + D_V \frac{\partial(N_V - N_V^{eq})}{\partial x} + (1 - N_V)v, \end{aligned} \quad (18)$$

$$\Omega J_V = \Omega j_B + N_V v = \frac{N_V D_V}{kT} \left(Ze\rho j_x - \Omega \frac{\partial \sigma}{\partial x} \right) - D_V \frac{\partial(N_V - N_V^{eq})}{\partial x} + N_V v, \quad (19)$$

$$N_V - N_V^{eq} \ll N_V^{eq} \text{ (typically)} \Rightarrow N_V^{eq} = \exp\left(-\frac{E_V - \sigma\Omega}{kT}\right), \quad (20)$$

$$\Omega J_V + \Omega J_B = 0, \quad (21)$$

$$\frac{\partial N_V}{\partial t} = -\frac{\partial}{\partial x}(\Omega J_V) - \frac{(N_V - N_V^{eq})}{\tau_V} \approx 0, \quad (22)$$

$$\frac{\partial \sigma}{\partial t} = -\frac{K}{3} \frac{\partial v}{\partial x}, \quad (23)$$

$$N_V D_V \approx D^*. \quad (24)$$

Very similar case was analyzed by Kirchheim in 1992 [29], but he did not use the sinks-source term for calculation of lattice drift.

4. Electromigration in two-phase alloy (solder) under condition of local quasi-equilibrium between phases

The magnitude and direction of the current were proved to have a strong influence on the phase composition of the diffusion zone and on the growth kinetics of phase layers. The influence of the electric field on phase formation in the diffusion zone was found e.g. in Au–Al, Cu–Sn and CaO–Al₂O₃ systems [25]. In this section, we distinguish the purely diffusional stage of the influence of the external electric field on phase formation process. The model describes the case when thermodynamically allowed phases have already appeared and continue growing in the diffusion zone.

Let us consider the two-phase fine-grained alloy (mixture) $\alpha + \beta$ with small solubility of A in β -phase and of B in α -phase. The main equations for interdiffusion fluxes in the bi-velocity form (which includes the Darken drift of the material) are

$$J_A = c_A B_A \left(F_A^{ext} + \Omega_A \frac{\partial \sigma}{\partial x} \right) + c_A v, \quad (25)$$

$$J_B = c_B B_B \left(F_B^{ext} + \Omega_B \frac{\partial \sigma}{\partial x} \right) + c_B v. \quad (26)$$

Here, F_B^{ext} has different interpretations for different external driving forces. For example [30], in case of electromigration, $F_B^{ext} = z_B e \rho j$ (Z_B is a partial effective charge of B ions under electron wind), in case of thermomigration, where Q_B is a partial heat of transport for B atoms. In the case of artificial gravitation (e.g. centrifuge), $F_B^{ext} = m_B g = m_B \omega^2 R$.

Multiplying Equations (25) and (26) by corresponding atomic volumes, we obtain equations in terms of volume fractions ($f_A + f_B = 1$):

$$f_A = \Omega_A C_A, \quad (27)$$

$$f_B = \Omega_B C_B. \quad (28)$$

Summation of (27) and (28) together with constraint of fixed volume gives:

$$\begin{aligned} 0 &= \text{div}(\Omega_A J_A + \Omega_B J_B) = \frac{\partial}{\partial x} (\Omega_A J_A + \Omega_B J_B) \\ &= \frac{\partial V}{\partial x} + \frac{\partial}{\partial x} \left(f_A B_A F_A^{ext} + f_B B_B F_B^{ext} + f_A B_A \Omega_A + f_B B_B \Omega_B \frac{\partial \sigma}{\partial x} \right). \end{aligned} \quad (29)$$

Condition (29) in our one-dimensional problem with zero fluxes and gradients at infinities gives:

$$V = -(f_A B_A F_A^{ext} + f_B B_B F_B^{ext}) - (f_A B_A \Omega_A + f_B B_B \Omega_B) \frac{\partial \sigma}{\partial x}. \quad (30)$$

Substitution of Equation (30) into Equations (27) and (28) gives:

$$\Omega_B J_B = f_A f_B \left[B_B F_B^{ext} - B_A F_A^{ext} + (B_B \Omega_B - B_A \Omega_A) \frac{\partial \sigma}{\partial x} \right] \quad (31)$$

and to conservation of matter and volume,

$$\frac{\partial f_B}{\partial t} = -\frac{\partial}{\partial x} (\Omega_B J_B) = -\frac{\partial}{\partial x} \left[(1 - f_B) f_B B_B F_B^{ext} - B_A F_A^{ext} + (B_B \Omega_B - B_A \Omega_A) \frac{\partial \sigma}{\partial x} \right]. \quad (32)$$

On the other hand, divergence of drift velocity determines the rate of stress changes according to Equation (4). Combining Equations (4) and (13), one gets:

$$\frac{\partial \sigma}{\partial t} = \frac{K}{3} \frac{\partial}{\partial x} \left[f_A B_A F_A^{ext} + f_B B_B F_B^{ext} + (f_A B_A \Omega_A + f_B B_B \Omega_B) \frac{\partial \sigma}{\partial x} \right] \quad (33)$$

Equations (32) and (33) give a self-consistent set of coupled equations of Burgers type for atomic fraction and of diffusion type for stress. Exact solution can be obtained based on implicit difference methods for differential functional equations [31]. Numeric solution of these two coupled equations should give the time evolution of the spatial separation of phases and the redistribution of stresses. The computer implementation was based on the steady-state approximation for the stress. In such a case, Equation (33) becomes:

$$0 = \frac{\partial \sigma}{\partial t} = \frac{K}{3} \frac{\partial}{\partial x} \left[f_A B_A F_A^{ext} + f_B B_B F_B^{ext} + (f_A B_A \Omega_A + f_B B_B \Omega_B) \frac{\partial \sigma}{\partial x} \right], \quad (34)$$

thus

$$\frac{\partial \sigma}{\partial x} = -\frac{f_A D_A^* F_A^{ext} + f_B D_B^* F_B^{ext}}{f_A D_A^* \Omega_A + f_B D_B^* \Omega_B} = -\frac{f_A B_A F_A^{ext} + f_B B_B F_B^{ext}}{f_A B_A \Omega_A + f_B B_B \Omega_B}. \quad (35)$$

To solve the Equations (32) and (35), the standard numerical scheme was used; mainly the method of lines to solve numerically the ordinary differential equations (ODEs) system resulting from the space discretization [32]. The uniform grid, which contained N mesh points along the x direction, respectively, was used and the concentrations and drift velocity were defined at points x_k . The applied discretization led to the system of ODEs in time variable.

Then, the time integrator used in the present computations was based on Runge–Kutta method. Exactly, the adaptive step-size Runge–Kutta–Fehlberg modification was used. The six evaluations of the functions from the fifth-order Runge–Kutta algorithm were used to make other combinations implemented in the fourth-order Runge–Kutta method. The difference between these two estimates served as an estimate of the truncation error. Hence, the step size was adjusted [33].

The initial phase fractions are constant for every x . The steady-state pressure profile is presented in Figure 4.

During the time interval of getting to asymptotic regime, the two-phase zone evolves. On the left end of the material, the pure β -phase is accumulated (Figure 5). The magnitude of redistribution depends on the external force and the difference in components' atomic masses. During the asymptotic regime, all markers are immovable.

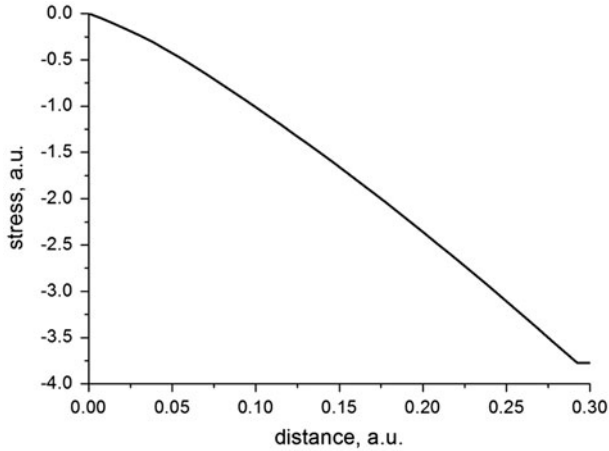


Figure 4. The nondimensional steady-state stress distribution.

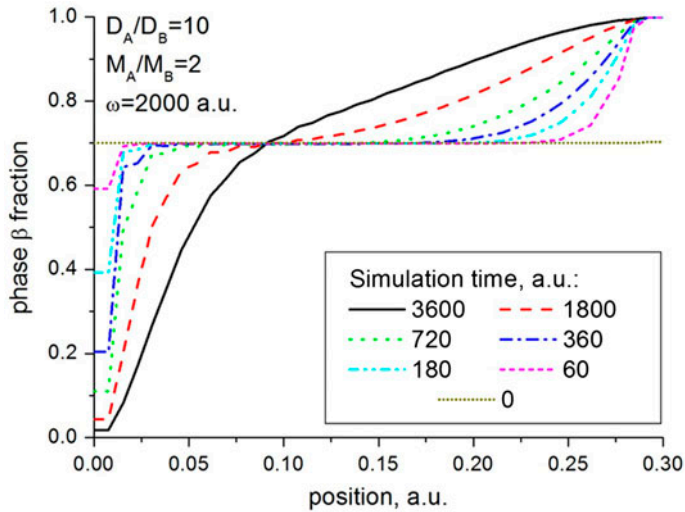


Figure 5. (colour online) The evolution of the phase fractions in the two-phase zone of the binary alloy during the sedimentation process.

5. Summary

Simultaneous action of backstress and of Kirkendall shift during electromigration in pure metals and in two-phase mixtures was described by self-consistent scheme.

The phenomenological model of electromigration in the two-phase alloy (solder) under condition of the local quasi-equilibrium between the phases was formulated. The mass transfer occurs under the combined mechanisms of the Kirkendall effect,

backstress and external force (sedimentation). The different models of electromigration in pure metals under the condition of quasi-equilibrium vacancies (unlimited power of vacancy sinks-sources) and electromigration in pure metal with account of nonequilibrium vacancies were presented.

In this work, we neglected an effect of vacancy concentration on molar volumes and the hydrostatic tension was approximated as one-third of the spur of stress tensor. The presented formalism can be extended to avoid above simplifications.

Acknowledgements

This paper is dedicated to the memory of Prof. Vitaliy Slezov, who passed away on October 30, 2013. His ideas and rigorous mathematical treatments of the diffusion-controlled first-order phase transformations kinetics (from nucleation to coarsening) are now classical. Discussions with him were very useful for better understanding the of stresses–vacancies–Kirkendall synergy. One of the authors (AG) is grateful to AGH University for hospitality, and also to the Ministry of Education and Science of Ukraine and to Ukrainian State Fund for Fundamental Research for partial support.

Funding

This work is supported by a National Science Center (Poland) decision number DEC-2011/02/A/ST8/00280.

Notes

1. Authors are not aware about such experiments with aluminum or copper lines.
2. We emphasize this since in some experimental papers authors use both Equations (6) and (7), and that is wrong.

References

- [1] L.S. Darken, *Trans. AIME* 174 (1948) p.184.
- [2] K.E. Schwarz, *Elektrolytische Wanderung in flüssigen und festen Metallen* (The electrolytic path in liquid and solid metals), J. A. Barth Verlag, Leipzig, 1940.
- [3] I.A. Blech, *J. Appl. Phys.* 47 (1976) p.1203.
- [4] I.A. Blech and C. Nabarro, *Appl. Phys. Lett.* 29 (1976) p.131.
- [5] K.N. Tu, J.W. Mayer and L.C. Feldman, *Electronic Thin Film Science for Electrical Engineers and Material Scientists*, Macmillan Publishing Company, New York, 1992.
- [6] K.N. Tu, *Solder Joint Technology: Materials, Properties and Reliability*, Springer, New York, 2007.
- [7] M. Abdulhamid, C. Basaran and Y.S. Lai, *IEEE Trans. Adv. Packag.* 32 (2009) p.627.
- [8] W. Yao and C. Basaran, *J. Appl. Phys.* 114 (2013) p.103708.
- [9] C. Basaran and M. Lin, *Int. J. Solids Struct.* 44 (2007) p.4909.
- [10] C. Basaran and M. Lin, *Mech. Mater.* 40 (2008) p.66.
- [11] C. Basaran and M.F. Abdulhamid, *Mech. Mater.* 41 (2009) p.1223.
- [12] W. Yao and C. Basaran, *J. Appl. Phys.* 111 (2012) p.063703.
- [13] A.D. Smigelskas, *Trans. AIME* 171 (1947) p.130.
- [14] J. Bardeen and C. Herring, *Diffusion in alloys and the Kirkendall effect*, in *Imperfections in Nearly Perfect Crystals*, W. Shockley, ed., Wiley, New York, 1952, p. 261.

- [15] K. Zeng and K.N. Tu, *Mater. Sci. Eng. R: Rep.* 38 (2002) p.55.
- [16] T.Y. Lee, K.N. Tu and D.R. Frear, *J. Appl. Phys.* 90 (2001) p.4502.
- [17] H. Gan, W.J. Choi, G. Xu and K.N. Tu, *JOM* 54 (2002) p.34.
- [18] K.N. Tu, *J. Appl. Phys.* 94 (2003) p.5451.
- [19] S.W. Liang, H.-Y. Hsiao, C. Chen, L. Xu, K.N. Tu and Y.-S. Lai, *J. Electron. Mater.* 38 (2009) p.2443.
- [20] J.W. Nah, F. Ren, K.N. Tu, S. Venk and G. Camara, *J. Appl. Phys.* 99 (2006) p.023520.
- [21] H. Ye, C. Basaran and D.C. Hopkins, *Int. J. Solids Struct.* 40 (2003) p.4021.
- [22] M. Lin and C. Basaran, *Comput. Mater. Sci.* 34 (2005) p.82.
- [23] X.F. Zhang, J.D. Guo and J.K. Shang, *Scr. Mater.* 57 (2007) p.513.
- [24] Y.D. Lu, X.Q. He, Y.F. En and X. Wang, *Adv. Mater. Res.* 44–46 (2008) p.905.
- [25] Ch Chen, H.M. Tong and K.N. Tu, *Annu. Rev. Mater. Res.* 40 (2010) p.531.
- [26] M. Pharr, K.Z. Zhao, Suo Fan-Yi Ouyang and P. Liu, *J. Appl. Phys.* 110 (2011) p.083716.
- [27] V.V. Turlo, A.M. Gusak and K.N. Tu, *Philos. Mag.* 93 (2013) p.2013.
- [28] B. Wierzba and M. Danielewski, *Philos. Mag.* 91 (2011) p.3228.
- [29] R. Kirchheim, *Acta Metall. Mater.* 40 (1992) p.309.
- [30] A.M. Gusak, Y.A. Lyashenko, S.V. Kornienko, M.O. Pasichnyy, A.S. Shirinyan and T.V. Zaporozhets, *Diffusion-controlled Solid State Reactions in Alloys, Thin-Films, and Nano systems*, Wiley VCH, Berlin, 2010.
- [31] L. Sapa, *Zeitschrift für Analysis und ihre Anwendungen* 32 (2013) p.313.
- [32] W.E. Schiesser, *The Numerical Method of Lines*, Academic Press, San Diego, CA, 1991.
- [33] W.H. Press, B.P. Flannery, S.A. Teukolsky and W.T. Vetterling, *Numerical Recipes in C: The Art of Scientific Computing*, Cambridge University Press, New York, 1992.